Detection of corrosion beneath a paint layer by use of spectral polarization optical imaging

J. H. Ali, W. B. Wang, P. P. Ho, and R. R. Alfano

Institute for Ultrafast Spectroscopy and Lasers and New York State Center for Advanced Technology for Ultrafast Photonics Materials and Applications, Department of Physics, The City College and Graduate School of the City University of New York, New York, New York 10031

Received May 9, 2000

The spectral and polarization properties of scattered light were used to image corrosion beneath the surface of a painted aluminum plate. The quality of imaging of the corrosion on the metal surface was significantly enhanced by the spectral polarization optical imaging technique. Depolarization scattered light was used to detect and image corrosion beneath the paint layer. © 2000 Optical Society of America

OCIS codes: 260.5430, 290.1350, 290.7050, 110.3080, 120.4630.

Corrosion of a metal surface increases significantly as the structure ages. Structural defects from environmental interactions can cause failure owing to micromechanism fatigue. Detection of corrosion and cracks at the earliest stages is an important step toward improving safety and reducing cost. Aging aircraft experience increased structural failures as a result of corrosion. Several methods, such as x-ray,[1] ultrasonic,[2] and electrochemical phenomenon[3] approaches, are currently used to investigate corrosion. These methods have a limited capability and sensitivity, and thus corrosion cannot be discovered at the earliest stage. Detection of hidden corrosion in aircraft structures by ultrasound techniques gives poor spatial resolution and imaging contrast near the surface region.

The ability to image corrosion beneath paint is limited by light reflection, absorption, and scattering from the paint. Photons propagating in turbid media have their incident direction, polarization, and phase randomized by multiple scattering. The photons can be viewed as being divided into ballistic, snake, and diffusive components.[4] The ballistic or coherent component results from the photons that travel the shortest path in a turbid medium, whereas diffusive or incoherent photons travel a larger distance than do ballistic or snake photons. The degree of depolarization depends on the initial polarization state, the number of scattering interactions, the anisotropy of each scatter, and the properties of the surrounding medium. Photonic techniques offer a rapid and easy approach to detection of corrosion *in situ*. Various defects in a highly scattering medium at certain depths can be detected with an optical technique[5] based on the spectral and polarization properties of the scattered light from a turbid medium. In this Letter we report the use of spectral and polarization dependence of the far-red and near-infrared scattered light to detect corrosion on a metal surface beneath a highly scattering turbid paint layer.

Understanding the underlying light propagation in highly scattering color paint will help to improve imaging of objects beneath the paint. Wavelengths in the far-red and the near-infrared ranges can penetrate paint layers and can be used to investigate corrosion beneath paint. Reflected and backscattered light from different species and locations in matter have different degrees of polarization.

Paint is a pigmented liquid composition that is composed mainly of TiO_2 and other chromophores placed in a binder, which is converted into a solid film after application as a thin layer. The function of TiO_2 is to scatter light, and it provides brightness and opacity. In general, the color of paint is a function of the absorption constant of the chromophore, the refractive index, and the particle size. Figure 1 shows the trajectories of the incident and the scattered light from a painted metal surface with corrosion.

The sample used in our experiment was an aluminum plate with a circular area of corrosion of ~2-cm diameter. Corrosion was induced by the reaction of a base solvent of potassium hydroxide with the surface of the aluminum plate for ~24 h. It is well known that a uniform corrosive layer can be created when a metal plate is soaked in a corrosive solution, such as an acid or a base. Mass loss W as a function of soaking time t of the sample in an acid solution is given by $W = At^N$, where A and N are constants that are independent of the soaking time and $N > 1$ when active dissolution occurs.[6] A high value of N shows low corrosion resistance. A low value of A indicates high corrosion resistance. The corrosion rate is not constant but increases with soaking time. If we take $A = 5$ μg (high-corrosion-resistance material), $N = 1.2$, and $t = 24$ h, the calculated mass loss is ~30 mg. The thickness of the corrosion is 35 μm.

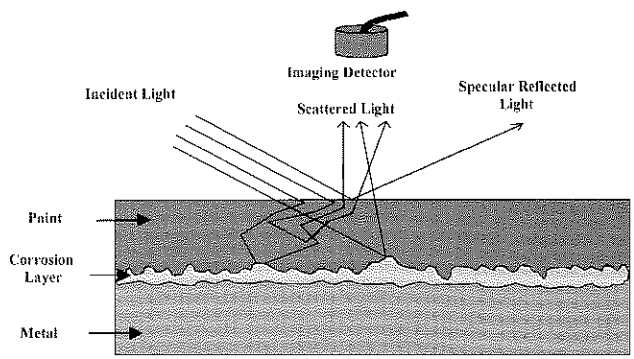

Fig. 1. Incident- and scattered-light rays from the paint–corroded-metal medium.

0146-9592/00/171303-03$15.00/0

The bottom half of the corrosion was painted with red paint of 40-μm thickness. The transmission curve of the red paint is shown in Fig. 2, which indicates that wavelengths greater than 600 nm are transmitted. The corrosion beneath the red paint cannot be seen visually or with a conventional camera, as shown in the inset photograph of Fig. 3.

When a linearly polarized light is incident upon the painted metal, the state of the backscattered and reflected light from the surface is partially polarized, whereas the light that is scattered from within the coating is depolarized. The degree of polarization of the scattered light decreases when the distance that the light travels through the scattering medium increases. As a result the polarization status of the light can be used for imaging corrosion or cracks at different depths beneath paint. The degree of polarization is defined as

$$D = (I_{\parallel} - I_{\perp})/(I_{\parallel} + I_{\perp}), \quad (1)$$

where $I_{\parallel}$ and $I_{\perp}$ are the intensities of the parallel and the perpendicular components, respectively, of the light that is reflected or scattered from the object. The contrast is the difference in light intensity in an object or image and is defined as

$$C = (I_{\max} - I_{\min})/(I_{\max} + I_{\min}), \quad (2)$$

where $I_{\max}$ and $I_{\min}$ are the maximum and minimum intensities of light recorded from the object, respectively.

The experimental arrangement for detecting the corrosion beneath the paint by use of the spectral polarization imaging technique is shown in Fig. 3. A beam of a white light of diameter ~2.5 cm is used to illuminate the sample. Wideband filters from 600 to 900 nm are alternatively used to select the desirable spectral range of the illumination and the detected light. A polarizer (P_1) located in the incident-light beam pathway yields linearly polarized illumination light with its polarization oriented parallel or perpendicular to that of the second polarizer orientation. The second polarizer (P_2) is positioned in front of the CCD camera for selection of the direction of detection polarization. A cooled CCD camera (Photomatrix CH250) equipped with a zoom lens of 50-mm focal length is used to record the images. The wavelength and polarization dependence of the scattered-light images are tested by a change of the illumination wavelength (600–900 nm) and rotation of the first polarizer (P_1).

A circular corroded sample with its bottom part covered by a painted layer as shown in Fig. 3 was imaged. Figures 4(a), 4(b), and 4(c) show parallel scattered-light images recorded at different excitation wavelengths (600, 700, and 800 nm, respectively) in the parallel polarization configuration. Figures 4(d)–4(f) show perpendicular scattered-light images recorded at the same excitation wavelengths, in the perpendicular polarization configuration.

It is clear from Fig. 4 that the intensity of the scattered light from the bottom half of the circular corrosion increases as the wavelength increases in both the parallel and the perpendicular states. This observation can be understood in terms of the fact that transmission of the red paint at 800 nm is higher than that at the shorter wavelengths, such as 600 and 700 nm, as shown in Fig. 2. As the wavelength gets longer the penetration gets deeper, and so more information can be obtained from the corrosion beneath the paint layer. Similar results were obtained for blue paint, in which the onset of the transmission wavelength is greater than 700 nm.

A short wavelength such as 600 nm cannot reach the corrosion layer. In this case the resulting images are formed from photons that are scattered from the surface or subsurface (smaller than 40 μm) of the paint medium. On the other hand, the longer wavelengths (700 and 800 nm) with a greater penetration had a better chance to pass through the paint medium

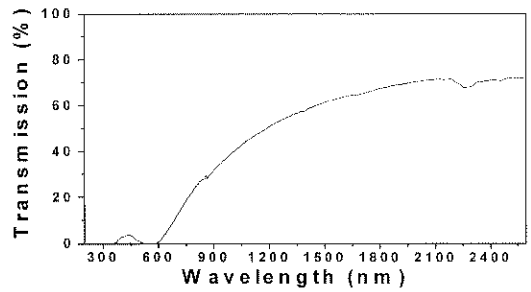

Fig. 2. Transmission curve of red paint in the wavelength range from 200 to 2500 nm.

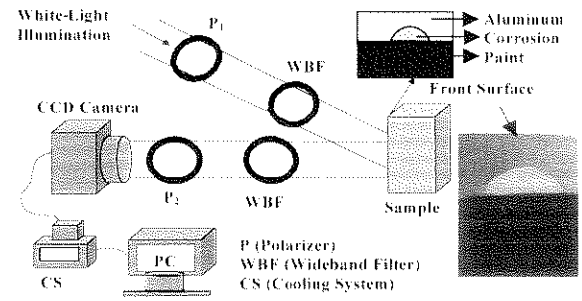

Fig. 3. Experimental setup: PC, personal computer.

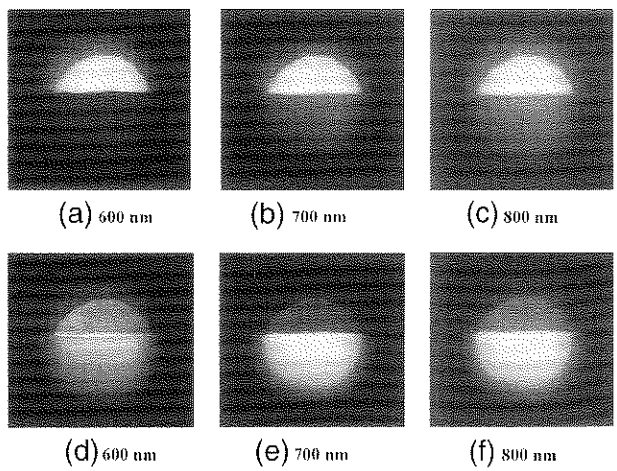

Fig. 4. Images of corrosion on the top of an aluminum plate, obtained by use of spectral and polarization properties. The bottom half of the circular corrosion and the aluminum plate are painted red. (a)–(c) parallel polarization images, (d)–(f) perpendicular polarization images.

Table 1. Degree of Polarization of the Images

	Wavelength (nm)		
Location	600	700	800
Top, unpainted corroded half	0.79	0.82	0.74
Bottom, painted corroded half	0.50	0.12	0.06

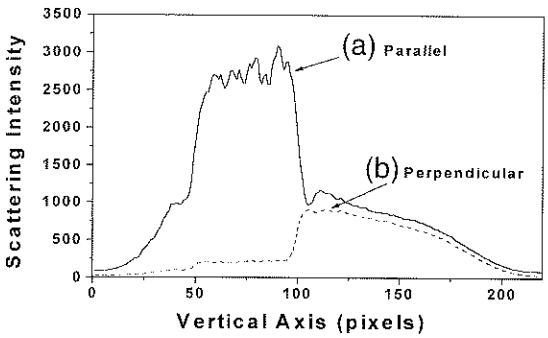

Fig. 5. Digitized intensity profiles for 700 nm along the vertical axis at the center of (a) the parallel polarization image [Fig. 4(b)] and (b) the perpendicular polarization image [Fig. 4(e)].

to reach the corrosion beneath the paint. The distortions in the corrosion layer cause the light to scatter in all directions. Since the CCD camera is fixed along the normal of the sample surface, the reflected light from the paint surface is specularly reflected to the right-hand side of the CCD camera. In Figs. 4(a)–4(c), the intensity of the scattered light from the top, unpainted half (low-scattering surface) is stronger than that of the bottom, painted half. Large portions of the scattered photons from the top half are registered in the CCD in the parallel polarization configuration, whereas a small portion of the scattered photons from the corrosion beneath the paint are registered in the CCD camera in the parallel configuration, owing to scattering (which dominates in the long-wavelength region) and absorption (which dominates in the short-wavelength region) in the paint medium. The multiple-scattering processes through the bottom half cause the scattered light to be depolarized. Absorption in the paint medium is very high in the short-wavelength region, for example, at 600 nm [see Fig. 4(a)].

In Figs. 4(d), 4(e), and 4(f), the intensities of the perpendicular scattered light from the bottom half of the corrosion at 600, 700, and 800 nm, respectively, are higher than those of the scattered light from the top half. The photons from the bottom half are scattered in all directions as in the top half, but paint molecules depolarize the photons more in the bottom half. A large portion of these photons is registered in the CCD camera in the perpendicular configuration. Most of the scattered photons from the top half are still highly polarized in the parallel configuration, and a very small portion is registered in the CCD camera in the perpendicular configuration. The scattering signal in the perpendicular configuration from the bottom half is stronger than that from the top half, as shown in Figs. 4(d)–4(f). This observation is confirmed by the degrees of polarization in the two areas, as shown in Table 1.

The degree of polarization of the images in Fig. 4 at different wavelengths can be calculated with Eq. (1). The calculated results, shown in Table 1, indicate that as the wavelength gets longer the degree of polarization gets smaller in the bottom half. This can be understood as happening because the scattered signal from the 800-nm photons is coming from a region deeper than that from the 600- or the 700-nm photons. As the degree of polarization gets smaller, the corrosion beneath the paint appears when the depolarized component is used. The degree of polarization in the top half is high and does not change much with the wavelength in the 600–800-nm region, as shown in Table 1.

It can be seen from Fig. 4 that the image contrast of the painted corrosion over the unpainted corrosion for perpendicular images is much better than that for the parallel images at each wavelength. The improvement of the perpendicular corrosion images over the parallel images can be seen more clearly in the digitized intensity profiles. Vertical scans from top to bottom in the middle of the images in Figs. 4(b) and 4(e) were taken for digitization purposes. In Fig. 5, curves (a) and (b) represent the intensity distributions of the parallel and the perpendicular polarization images of Figs. 4(b) and 4(e), respectively. The image contrasts of Figs. 4(b) and 4(e) (compare the top and bottom portions) were calculated with Eq. (2), and the digital data were obtained from Fig. 5. The calculated results show that the contrast of the perpendicular image (0.62) is ~1.5 times higher than that of the parallel image (0.40).

In conclusion, far-red and near-infrared spectral polarization imaging has been used to image corrosion hidden beneath a highly scattering medium of paint. Depolarized scattered-light imaging is preferable to the use of the parallel image configuration for detecting an object embedded in a turbid medium.

This Letter was developed under the auspices of the City University of New York Center for Advanced Technology for Ultrafast Photonic Materials and Applications, a New York State Center for Advanced Technology supported by the New York State Science Technology and Academic Research Program.

References

1. D. Wang, C. Cao, L. Zhang, and H. Lin, Corrosion **46,** 975 (1990).
2. M. de Billy, F. Cohen-Tenoudji, A. Jungman, and G. J. Quentin, IEEE Trans. Sonics Ultrason. **SU-5,** 356 (1976).
3. M. Stratmann and H. Streckel, Corros. Sci. **30,** 681 (1990).
4. L. Wang, P. P. Ho, C. Liu, G. Zhang, and R. R. Alfano, Science **253,** 769 (1991).
5. W. B. Wang, S. G. Demos, J. H. Ali, G. Zhang, and R. R. Alfano, Opt. Commun. **147,** 11 (1998).
6. C. Weiping and X. Chenghui, J. Mater. Sci. Lett. **16,** 113 (1997).